Cement and Concrete Research 38 (2008) 1416–1423

Contents lists available at ScienceDirect

Cement and Concrete Research

journal homepage: http://ees.elsevier.com/CEMCON/default.asp

Experimental study of mechanical behaviour of cement paste under compressive stress and chemical degradation

S.Y. Xie, J.F. Shao *, N. Burlion

Laboratoire de Mécanique de Lille, UMR 8107 CNRS, Polytech-Lille, Cité scientifique, Villeneuve d'Ascq, France

ARTICLE INFO

Article history:
Received 7 January 2008
Accepted 26 June 2008

Keywords:
Calcium leaching
Chemo-mechanical coupling
Cement paste
Concrete
Chemical damage

ABSTRACT

This paper presents experimental investigations of mechanical behaviour of a pure cement paste subjected to compressive stresses and chemical degradation. Two series of laboratory tests have been performed: decoupled and coupled chemical-mechanical tests. Hydrostatic and triaxial compression tests have first been realized respectively on sound and chemically degraded samples. The obtained results allow the characterization of basic mechanical responses of the tested cement paste and the identification of chemical degradation effects on the mechanical behaviour. In the coupled tests, the samples are simultaneously subjected to deviatoric stresses and chemical leaching by aggressive solution flow. Variations of deformation of cement paste samples are measured during chemical degradation process. The results obtained in these tests can be used for the validation of chemo-mechanical constitutive modelling.

1. Introduction

Cement-based materials are largely used in different engineering constructions. Stability analysis of these structures requires the understanding and modelling of mechanical behaviours under complex multi-axial loading conditions. Depending on the level of applied stress, the basic mechanical behaviour of cement-based materials is generally characterized by coupled plastic deformation and damage by growth of microcracks. However, in many situations, these materials are subjected not only to mechanical loading but also to chemical degradation when they are in contact with aggressive environmental conditions such as rain, sea water and acid fluids. More recently, in the framework of sustainable developments, it is of great importance to study the feasibility of storage of radioactive wastes and other residual gas such as CO_2 in geological formation. The cement-based materials may be used as engineered barrier for such structures. It is clear that the durability analysis of these structures requires the characterization and modelling of long term behaviour of cement-based materials subjected to mechanical loading and chemical degradation.

For this purpose, a number of research works have been conducted on experimental investigation and numerical modelling of chemical degradation of cement-based materials [1–11], just to mention a few. These works have been devoted to various features of chemical degradation such chemistry equilibrium, calcium dissolution process, diffusion phenomenon, kinetics of degradation, factors influencing chemical degradation and consequences on mechanical behaviour and transport properties.

According to these investigations, the chemical degradation of cement-based materials is essentially controlled by two processes, the dissolution of different hydrate phases and diffusion of dissolved species inside interstitial fluid. The calcium dissolution mainly concerns Portlandite and various C–H–S phases, which provide the major part of macroscopic mechanical cohesion and strength of materials. The kinetics of chemical degradation is influenced by microstructure (compositions) of materials, chemical nature and temperature of aggressive solution, as well as pressure gradient of interstitial fluid. On the effects on mechanical behaviour, the chemical degradation leads to an increase of material porosity, and then affects elastic-plastic behaviours and transport properties (diffusivity, permeability).

However, most of the previous investigations have been focused on brittle behaviour of cement-based materials subjected to mechanical damage par microcracks and chemical degradation. Further, on the laboratory investigations, uncoupled chemical-mechanical tests were generally performed. Very few coupled laboratory tests are available. In the present work, the focus is put on the investigations of mechanical behaviour and chemical leaching of porous cement paste under compressive stresses including the transition from brittle to ductile behaviours. In particular, original coupled tests will be performed in which samples are simultaneously subjected deviatoric stresses and chemical leaching. The present paper is organized as follows: after the presentation of laboratory testing procedure and sample preparation, the basic mechanical behaviour of a pure cement paste is studied through hydrostatic and triaxial compression tests. Then the samples are immersed into aggressive solution for chemical leaching and mechanical tests are performed on fully degraded samples. Effects of chemical degradation on mechanical behaviours

---

* Corresponding author.
E-mail address: jian-fu.shao@polytech-lille.fr (J.F. Shao).

0008-8846/$ – see front matter © 2008 Elsevier Ltd. All rights reserved.
doi:10.1016/j.cemconres.2008.06.011

are identified. In the last part, coupled tests will be presented, in which aggressive solution is injected into sample under various deviatoric stress levels.

2. Experimental procedures

In this section, we present the experimental procedures used for preparation of chemically degraded samples and chemo-mechanical tests.

2.1. Samples preparation and chemical degradation

All the tests have been performed on a pure cement paste which is made at a water/cement ratio 0.44 in cylindrical moulds (diameter 36 mm and height 100 mm), using an G class Portland cement. The chemical compositions of the cement used are shown in Table A1 (Appendix 1). The demoulding was done after 24 h, then the cement paste were cured for 27 days immersed in water saturated with lime at 20 °C. After curing, the samples were cut with the height/diameter ratio 1.2 and 2.0. And then some of samples with the slenderness 2 were stored in saturated lime water until they were used in coupled tests, the others were immersed in the 6 mol/l of ammonium nitrate solution with a (cement/solution) volume ratio of 1:10 until the mechanical tests could be performed. Due to its high leaching capacity and strong aggressive character, the ammonium nitrate solution is largely used in cement-based materials in order to obtain fast decalcification ([3,6,12]). According to the studies conducted by Carde [12], there are many similarities between the degradation by pure water and that by ammonium nitrate solution in terms of dissolution of Portlandite, de decalcification of C–H–S phases and then the modification of material microstructure. In particular, in both cases, the kinetics of degradation may be described by a linear relation between the depth of degraded front and square root of time in the form [12,13,14]: $x_d(\mathrm{mm}) = a\sqrt{t(\mathrm{day})}$. Different values of the parameter α, which controls the kinetics of chemical degradation, may be found as functions of chemical nature of aggressive solution.

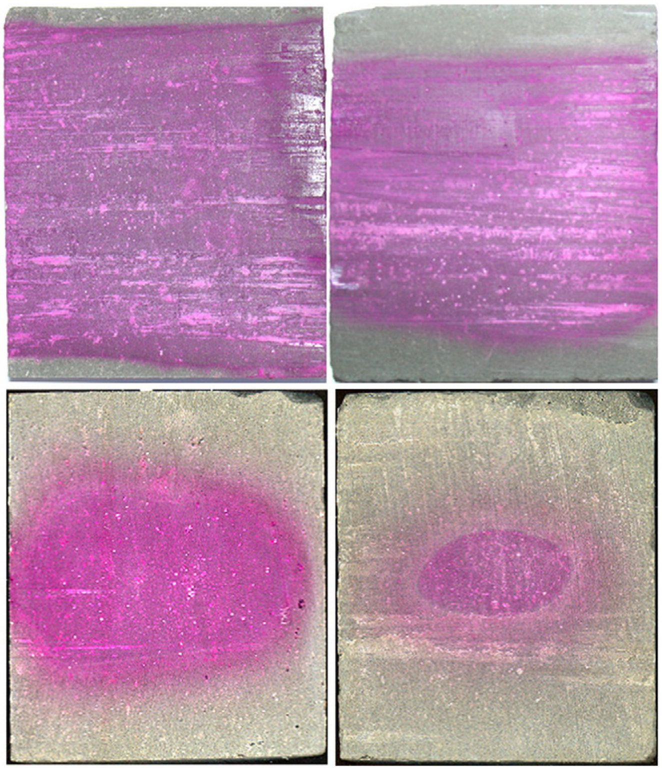

Fig. 1. Propagation of Portlandite dissolution front along longitudinal sections at different instances (after 1, 10, 28 and 53 days of degradation).

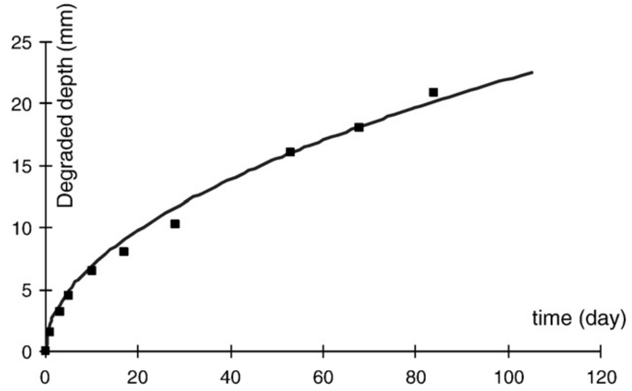

Fig. 2. Propagation of dissolution front with time — comparison between measured and calculated (continuous line) values.

For the estimation of this kinetics parameter, the samples with the ratio $H/D = 1.2$ are immersed in the ammonium nitrate solution with the concentration of 6 mol/l. At different time of degradation, the specimens shown in Fig. 1 are longitudinal sections. At first, the degraded specimen is taken out from the nitrate solution, and then it is cut along the longitudinal section, the surface is cleared with water and is dried with absorbent paper; the surface are then sprayed with phenolphthalein. Fig. 1 shows the progression of the Portlandite dissolution fronts at different instances of degradation namely, 1, 10, 28, 53 days. However, one can note that at the first instances, the penetration of degradation front is faster from the up and bottom surfaces than from the lateral surface. This phenomenon is probably due to the fact the immersed specimen were cut from longer cylinder samples with the same diameter. As a consequence of the fact, the up and bottom surfaces are fresh ones and the cutting may also generate some microcracks. At the same time, on the lateral surface which is not fresh, there may be is the formation of some protection layer with carbonation. Therefore, the lateral surface has smaller permeability and diffusivity regarding the penetration of degradation front. From the results obtained, it is found that the kinetics of degradation of cement paste in the present case may be approximated by $x_d(\mathrm{mm}) = 2.2\sqrt{t(\mathrm{day})}$. This means that the leaching front may reach the sample center after about 84 days of degradation (the sample height being 42 mm and the diameter being 36.1 mm). Fig. 2 shows the comparison between measured and calculated values of the dissolution front with time. In Fig. 3, the relative weight loss of samples and the change of pH degree of the solution are presented.

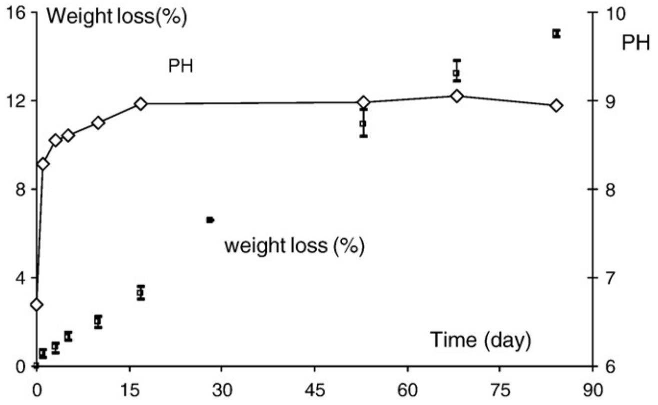

Fig. 3. Relative weight loss of cement paste samples and variation of pH of the solution with time.

Fig. 4. Surface difference between sound and chemically degraded cement paste samples.

The chemical degradation is initiated by the loss of chemical equilibrium between solid skeleton and acid interstitial solution at the boundaries of sample in contact with aggressive solution. One can see that during a first stage, the pH value of the solution increases very quickly reaches about 9 after a few days. Then the increase of pH value becomes slower and progressively reaches a quasi stationary value. In concordance with the thermodynamic equilibrium curve between calcium concentration in interstitial solution and that in solid skeleton as that established by Berner [2], the quick increase of pH value in the first stage may correspond to fast dissolution of Portlandite crystals. On the other hand, the weight loss of cement samples continuously increases with the time during the leaching process.

The change in porosity of cement paste due to chemical leaching was also studied. For this, sound and degraded samples were dried at the temperature of 105 °C. The porosity is calculated by simple comparison between dried samples and fully water saturated samples. It is shown that the porosity of the cement paste is significantly increased by the process of calcium dissolution, from 36% for the sound material to 60% for the degraded one in which the dissolution front reached the sample center, and the uniformly degraded depth covered about 74% of the diameter. These results clearly show that the degraded cement paste is a strongly porous material and its high porosity should have important impact of the mechanical behaviour of material. Figs. 4 and 5 show the general features of the top surface and a vertical section cut along diameter, respectively for the sound and degraded samples after the drying. The drying process generally induces volumetric shrinkage in cement paste. One can see that this shrinkage is much more important in the degraded material than in the sound one; this may be related to the pore collapse phenomenon in the degraded material due to its high porosity. Further, the partially degraded sample is a heterogeneous composite with a degraded zone and a sound core at the center. The two zones have different properties to the drying shrinkage; i.e. the shrinkage is higher in the degraded zone than that in the sound zone. As a consequence, there is a kinematical restraint for the drying shrinkage of the degraded zone. This may be the origin of initiation and propagation of microcracks in the degraded zone, as shown in Fig. 5.

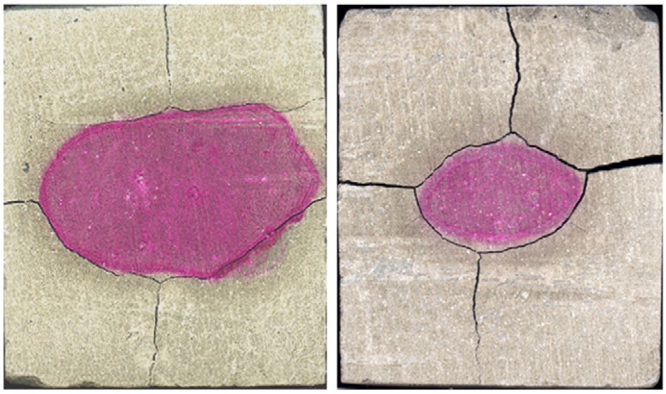

Fig. 5. Difference of a cut cross section between chemically degraded cement paste samples at different degradation states.

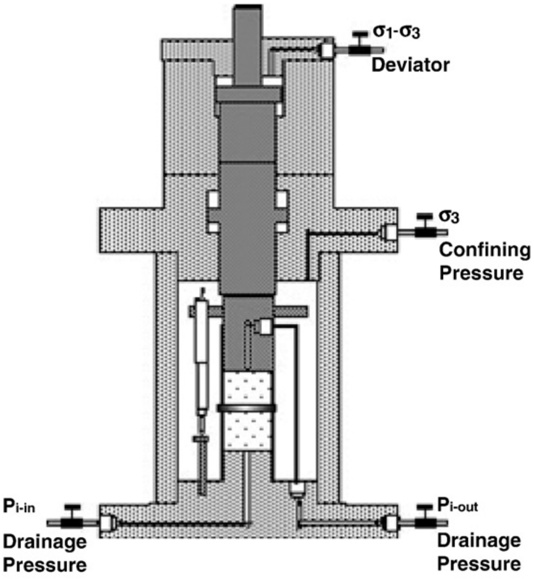

Fig. 6. Schematic presentation of the auto-compensated and auto-equilibrated triaxial cell.

Based on the XRF analysis, Heukamp et al. [7] showed that the Portlandite dissolution front reached the sample center after 9 days (the diameter being 11.5 mm), and uniformly calcium leached samples were obtained after about 45 days. Comparing with these results, it is expected to obtain uniformly calcium leached samples after about 450 days in the present case. Therefore, the chemically degraded samples used in this work were immersed in aggressive solution for about 2 years.

2.2. Experimental setup for mechanical and coupled tests

Three types of tests are performed in this study: standard triaxial compressive tests for the sound samples and chemically degraded samples, and coupled chemical–mechanical tests. All the tests are conducted under drained conditions using an auto-compensated and auto-equilibrated triaxial cell system (a patent of the Lille University, France). This cell is schematically presented in Fig. 6. It is operated with three high-pressure generators with a maximum capacity of 60 MPa each, one for the deviatoric stress loading, the second one for the confining pressure application and the third one for interstitial fluid flow. There are four captures of pressure, respectively measuring confining pressure, deviatoric stress, and pore pressure. The axial displacement is measured with two LVDTs in the cell, and the lateral deformation is measured with a special strain ring which is equipped with a blade on which a full-bridge of four strain gages is installed. Note that during coupled chemo-mechanical tests, the sample is first subjected to a triaxial stress state, and then aggressive solution is injected into the sample. In order to follow local deformation at different positions of the sample, three strain rings for measuring the lateral deformation are placed at different levels along the height as shown in Fig. 7.

All the tests will be performed on saturated samples under drained conditions. Before being placed in testing cell, the samples are first saturated by immersion in lime water or in chemical solution under vacuum condition for 6 h. After being placed in the cell, the samples are again saturated by stationary fluid flow. In triaxial compression tests performed on sound and chemical degraded samples, the pore pressure

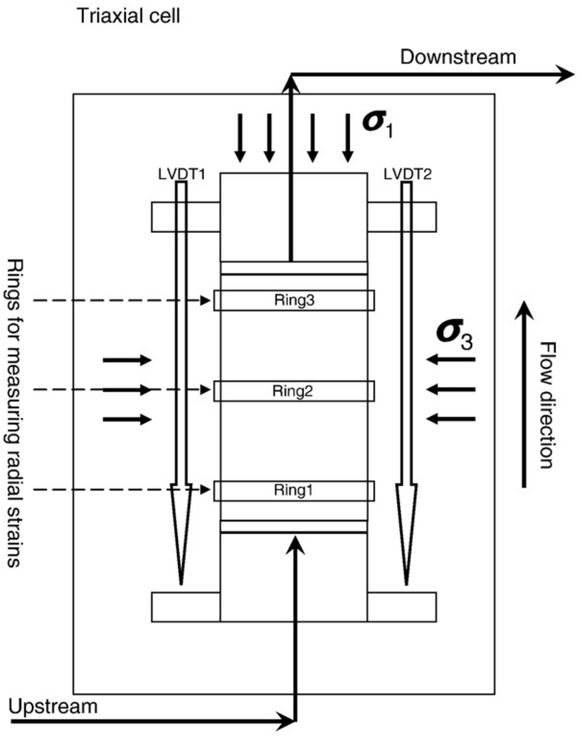

Fig. 7. Illustration of the system for measuring axial and lateral deformations.

at the inlet and outlet points are equal to atmospheric pressure. In coupled tests, a constant injection pressure is prescribed at the inlet point while the outlet pressure is equal to atmospheric pressure.

3. Basic mechanical behaviour of sound cement paste

As mentioned, above, the emphasis of the work is put on mechanical behaviour of cement paste under compressive stresses. The cement paste is a typical material with high porosity. In order to study its basic mechanical behaviour, a series of hydrostatic and conventional triaxial compression tests are performed on water saturated samples.

The drained triaxial compression test is realized in two stages. At the first, a confining pressure is applied to the sample in drained condition, and then kept to a constant value. In the second stage, the axial (deviatoric) stress is increased until failure or large strain in drained condition. Note that in order to keep a good saturation state, a constant pore pressure is maintained during the test.

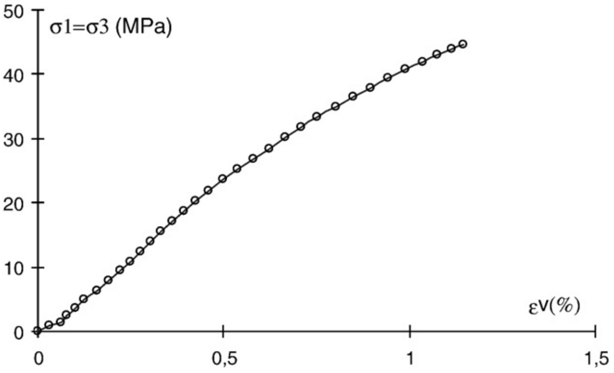

Fig. 8. Hydrostatic stress — volumetric strain curve of sound cement paste in hydrostatic compression test.

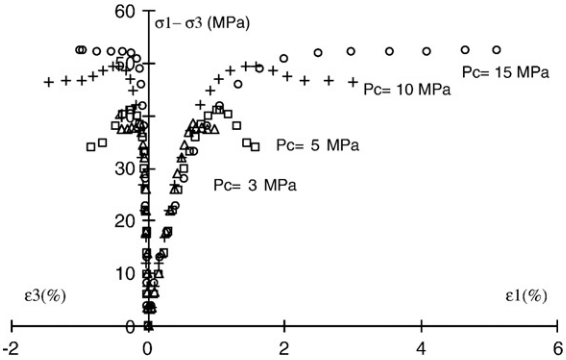

Fig. 9. Typical stress — strain curves of sound cement paste in triaxial compression tests with low confining pressures.

In the present work, seven triaxial compression tests with the confining pressures of 3, 5, 10, 15, 20, 30 and 45 MPa are carried out. For the test with 45 MPa confining pressure, the volumetric strain during hydrostatic compression phase is also measured and shown in Fig. 8. There is a quasi linear relation between hydrostatic stress and volumetric strain until a certain limit of stress. This linear response may correspond to elastic compaction of porous material. After the limit stress, say about 25 MPa, the stress–strain curve becomes progressively non linear and higher volumetric compaction rate is obtained. This emphasized volumetric strain may be due to inelastic pore collapse phenomenon, classically observed in porous materials. The limit stress can then be seen as the pore collapse threshold. Typical deviatoric stress, axial and lateral strains curves are shown in Figs. 9 and 10 for triaxial compression tests. First, one can observe a strong influence of the confining pressure on the mechanical responses of cement paste. Under low confining pressures (say 3, 5, 10 and 15 MPa), the basic behaviour of cement paste is elastic brittle or elastoplastic brittle. A peak deviatoric stress is obtained and this one significantly increases with the confining pressure. Sample failure is classically produced by the formation of localized shear bands. The orientation of shear bands depends on the value of confining pressure. Then there is a clear transition from brittle to ductile behaviour when the confining pressure increases. At high confining pressures (say 20, 30 and 45 MPa), no peak stress can be defined until relatively large axial strain; and the initial slope of stress versus axial strain curve is continuously increasing with confining pressure. This means that the applied deviatoric stress enhances pore collapse process. Accordingly, an important volumetric contraction is obtained. One of the specific features is that due to the high volumetric compressibility, the lateral strain at the beginning stage of deviatoric loading is smaller than that should be obtained in the linear elastic stage. Material failure may manifested by complete destruction of pore structure.

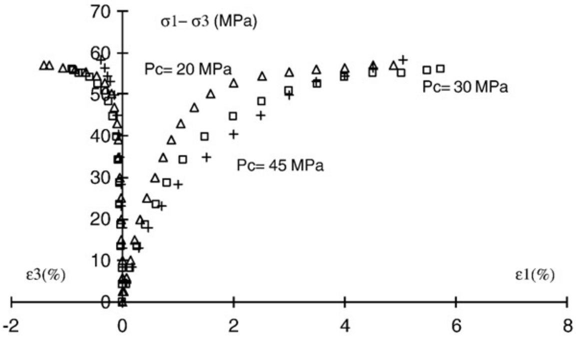

Fig. 10. Typical stress — strain curves of sound cement paste in triaxial compression tests with high confining pressures.

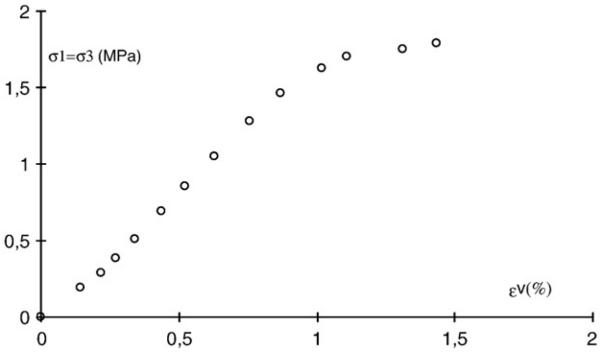

Fig. 11. Stress — volumetric strain curve of chemically degraded cement paste in hydrostatic compression test.

As a conclusion, the plastic deformation of porous cement paste may be characterized by two basic plastic mechanisms: plastic pore collapse mechanism dominating at high confining pressure and plastic shear process at lower confining pressure.

4. Mechanical behaviour of chemical degraded cement paste

In order to study the impact of chemical degradation on the mechanical behaviour of the cement paste, a series of hydrostatic and conventional triaxial compression tests are now performed on the fully degraded samples. For the reason of the strong degradation of the samples in order to avoid material failure by complete collapse of pore structure, the tests are carried out under low confining pressure only. Namely, five triaxial compression tests with the confining pressures of 0.1, 0.3, 0.6, 1.0 and 2.0 MPa have been carried out. Similar to the tests performed on the sound material, the volumetric compaction during the hydrostatic phase is measured for the test with 2.0 MPa confining pressure, as shown in Fig. 11. It is clear that due to important calcium dissolution state and high porosity, the pore collapse threshold of the degraded material is very low, say 1.5 MPa. Typical deviatoric stress–strains curves obtained in triaxial compression tests are presented in Figs. 12 and 13. As for the sound material, there is also a strong dependency of mechanical responses on the confining pressure. One finds again the clear transition from brittle to ductile behaviour when the confining pressure increases. Under low confining pressures (0.1 and 0.3 MPa), the basic behaviour of degraded cement paste is elastic brittle or elastoplastic brittle. A peak deviatoric stress is observed and increases with the confining pressure. At higher confining pressures (0.6, 1.0 and 2.0 MPa), there is no peak stress until large axial strain and there is significant volumetric compaction due to pore collapse phenomenon. Material failure is manifested by complete destruction of pore structure. The plastic deformation of the degraded material is also characterized by two mechanisms: deviatoric shearing and pore collapse.

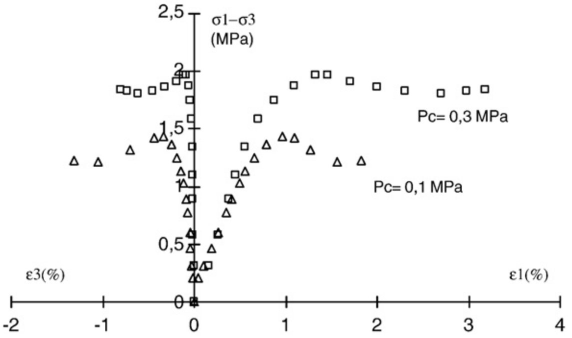

Fig. 12. Deviatoric stress — strains curves of chemically degraded cement paste in triaxial compression tests with low confining pressures.

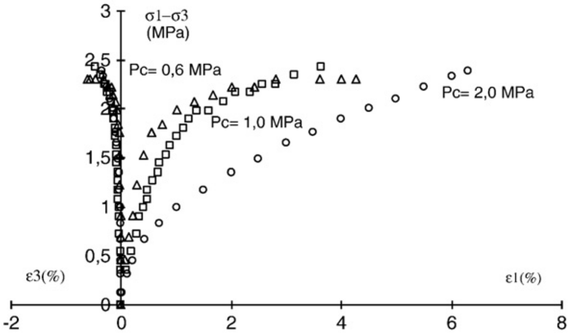

Fig. 13. Deviatoric stress — strains curves of chemically degraded cement paste in triaxial compression tests with high confining pressures.

However, behind these common features, the mechanical responses are strongly affected by the chemical degradation. In particular, the failure stress, the plastic yield stress in deviatoric shearing and the pore collapse yield stress are drastically reduced in the degraded cement paste. In Fig. 14, the plastic yield surfaces and deviatoric failure surface are presented in the *p*–*q* plane (mean stress versus deviatoric stress). The chemical degradation generates an important increase of material porosity, triggers a significant loss of strength and stiffness, and induces a higher pressure sensitivity of cement paste.

5. Coupled chemo-mechanical tests

In the investigations presented above, the impact of chemical degradation on the mechanical behaviour of cement paste is studied through comparing laboratory tests separately performed on sound and degraded samples. The results obtained can be used for the formulation and identification of chemo-mechanical constitutive models [15–19]. In these tests, mechanical loading and chemical degradation are uncoupled. However, in many practical applications, the cement-based materials are simultaneously subjected to mechanical loading and chemical degradation. Aggressive chemical solution penetrates into structure components with applied mechanical loads. One of the key concerns is to predict additional plastic deformation and variation of transport properties caused by chemical degradation. The purpose of coupled chemo-mechanical tests presented here is to investigate mechanical responses of cement paste during chemical degradation process. The results obtained in these tests may be used for the validation of chemo-mechanical models in typical boundary values problems.

The testing procedure is defined as follows: an initially sound sample is first subjected to a hydrostatic stress state and the deviatoric

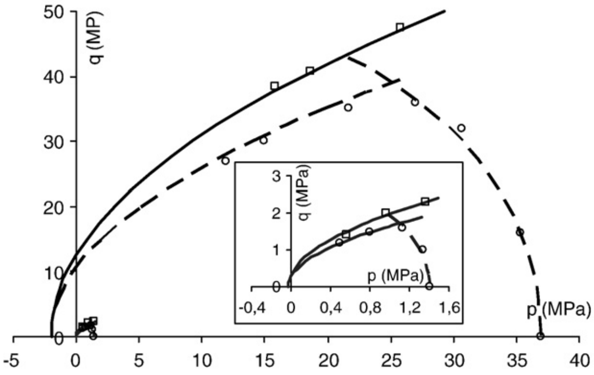

Fig. 14. Deviatoric and pore collapse yield surfaces and failure surface of cement paste — comparison between sound and chemically degraded materials (*p* being the compressive mean stress and *q* the deviatoric stress).

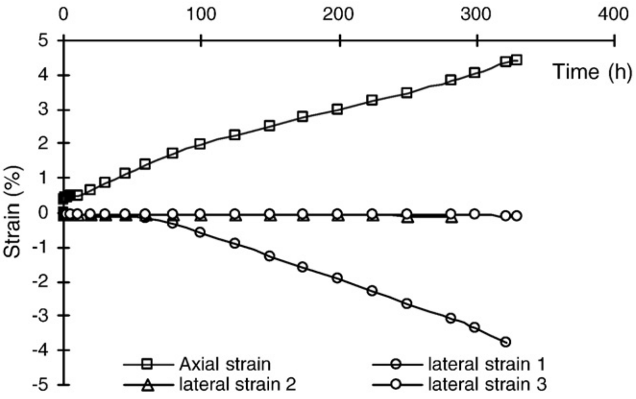

Fig. 15. Coupled chemo-mechanical triaxial test: evolutions of axial and radial strains during aggressive solution injection ($\sigma_3=5\ \mathrm{MP_a}$, $\sigma_1-\sigma_3=20\ \mathrm{MP_a}$, $\Delta p_{\mathrm{inj}}=2\ \mathrm{MP_a}$).

stress is then applied to a given value. Both the axial and radial stresses are maintained constant while an aggressive fluid is injected into the samples from the bottom face with a constant injection pressure. In this study, the ammonium nitrate solution with the concentration of 4 mol/l is used as aggressive agent. The average axial strain is calculated from the normalized average axial displacement ($\Delta U/L_0$) which is measured by the two LVDTs (Fig. 7). Lateral strains are monitored by the special strain rings during at three different levels along the height of sample (Fig. 7). This makes it possible to monitor the evolutions of lateral strains at these selected points during the progress of chemical degradation front. For a good distribution of the aggressive solution flow, two porous metal plates are placed on the top and bottom of the sample.

In order to understand the influence of the deviatoric stress on the mechanical behaviour in the coupled conditions, two coupled tests have been performed with the same confining pressure (5 MPa) and injection pressure (2 MPa), but two different deviatoric stresses (20 MPa and 8 MPa).

For the test with the deviatoric stress of 20 MPa, the initial height of the sample is 62 mm, and the distance between the rings and the bottom of the sample are, respectively, 6 mm for ring 1, 31 mm for ring 2 and 56 mm for Ring 3. The experimental results of the test are presented in Figs. 15 and 16. In Fig. 15, the average axial strain and lateral strains are presented as functions of injection time. Fig. 16 gives the variations of permeability of the sample and pH value of the leached solution collected at the outlet hole. In Fig. 17, a visual observation of the tested sample is shown.

For the test with a deviatoric stress 8 MPa, the height of the sample is 52 mm, and the distance between the rings and the bottom of the sample are, respectively, 10 mm for ring 1, 26 mm for ring 2 and 42 mm for ring 3. The experimental results of the test are presented in Figs. 18 and 19. Fig. 18 gives the average axial strain and lateral strains measured at three levels as functions of injection time. The variations of permeability of the sample and pH value of leached solution are shown in Fig. 19.

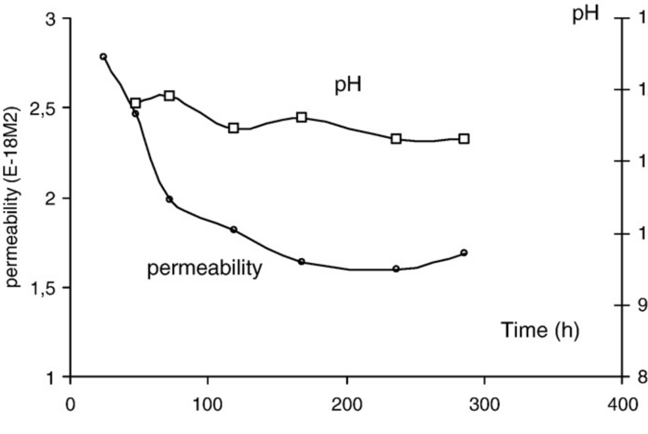

Fig. 16. Coupled chemo-mechanical triaxial test: changes in permeability and pH value during chemical fluid injection ($\sigma_3=5\ \mathrm{MP_a}$, $\sigma_1-\sigma_3=20\ \mathrm{MP_a}$, $\Delta p_{\mathrm{inj}}=2\ \mathrm{MP_a}$).

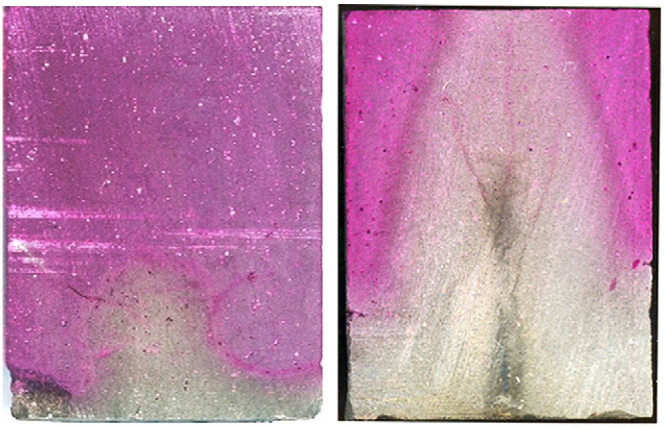

Fig. 17. Picture of longitudinal sections of tested sample in coupled triaxial degradation tests (left picture: $\sigma_3=5\ \mathrm{MP_a}$, $\sigma_1-\sigma_3=20\ \mathrm{MP_a}$, $\Delta p_{\mathrm{inj}}=2\ \mathrm{MP_a}$) and (right picture: $\sigma_3=5\ \mathrm{MP_a}$, $\sigma_1-\sigma_3=8\ \mathrm{MP_a}$, $\Delta p_{\mathrm{inj}}=2\ \mathrm{MP_a}$).

During the two coupled tests, the longitudinal permeability of sample as well as the pH value of leached solution at the outlet point is measured at different time of degradation. The sample permeability is determined using the steady-state flow method. During the tests, the interstitial pressure difference between the injection and outlet point is fixed to 2 MPa, and the flow volume of injected solution is monitored and the average flow rate calculated. Then the permeability is determined by applying Darcy's law.

From the results obtained, the following remarks can be drawn up.

1. For the test with the deviatoric stress of 20 MPa, one can see that the axial strain increases quasi linearly with time. The evolutions of the radial strains are in concordance with the propagation of chemical degradation front. The radial strain near the bottom of the sample (the ring N°1) begins to increase after 80 h injection, while the radial strains at the other two rings nearly do not evolve. Note that due to high deviatoric stress applied in this test, the chemically induced strains are clearly localized in the small zone near the

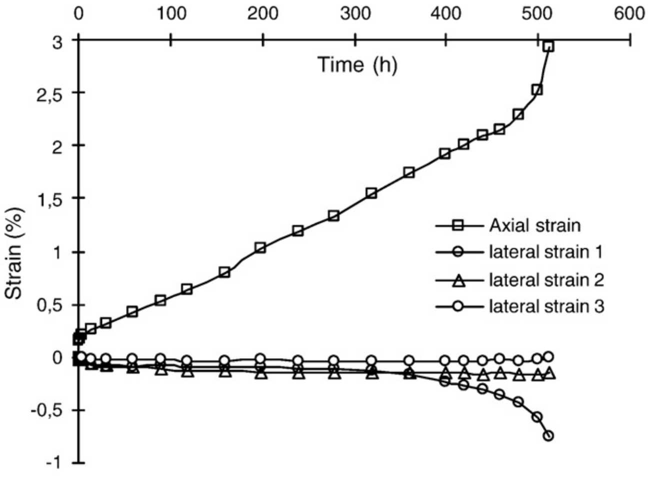

Fig. 18. Coupled chemo-mechanical triaxial test: evolutions of axial and radial strains during chemical fluid injection ($\sigma_3=5\ \mathrm{MP_a}$, $\sigma_1-\sigma_3=8\ \mathrm{MP_a}$, $\Delta p_{\mathrm{inj}}=2\ \mathrm{MP_a}$)

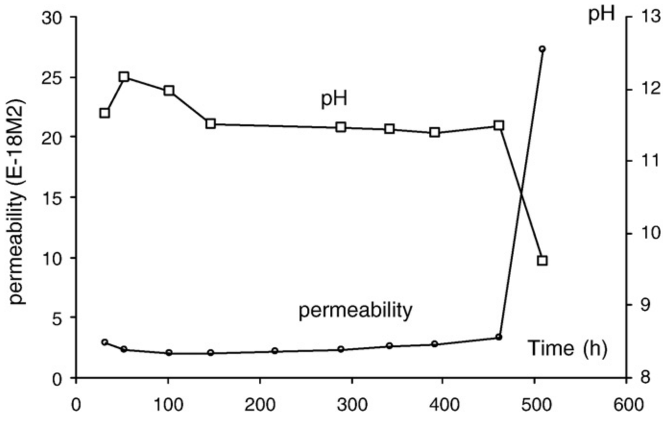

Fig. 19. Coupled chemo-mechanical triaxial test: changes in permeability during chemical fluid injection ($\sigma_3=5$ MP$_a$, $\sigma_1-\sigma_3=8$ MP$_a$, $\Delta p_{inj}=2$ MP$_a$).

bottom surface of the sample. When the test was stopped after more than 500 h, it seems that the chemical degradation front did not reach the middle height of the sample, as shown in Fig. 17. During this test, the permeability decreases in the first 150 h, and then it becomes constant. Note that in such a coupled test, there are two opposite factors affecting the material permeability. The increase of porosity issued from chemical leaching leads to the increase of permeability while the volumetric compaction due to applied mechanical loads may yield the decrease of material permeability. Therefore, a complex variation of permeability may be obtained in coupled tests.

2. For the test with deviatoric stress 8 MPa, the general trends are quite similar to those in the previous test. As that may be expected, the range of strains induced by chemical degradation is smaller because the applied deviatoric stress is smaller. There is a rapid increase of both axial and radial strain at the end of the test. It means an accelerated effect of chemical degradation. Further, the evolutions of radial strains at the middle and upper rings seem to be more significant than those in the previously test. However, in this test, the permeability decreases during the first 100 h, and then it increases slowly in the second stage, and finally, there is a rapid increase of the permeability. After the direct observation of the tested sample (Fig. 16b), there was the formation of a localized flow hole (wormhole) in the sample after 510 h injection, this may contribute directly to this sharp increase of permeability.
3. In the coupled test with the deviatoric stress of $\sigma_1-\sigma_3=20$ MP$_a$, there is a slight and regular decrease of pH value measured in the outlet interstitial solution (see Fig. 16). This could be due to partially incomplete chemical reaction between nitrate solution and solid calcium in cement paste. However, in the test with the deviatoric stress of $\sigma_1-\sigma_3=8$ MP$_a$, apart the similar slight decrease of pH value as the first test, there is a sharp diminution of pH value during the last stage of the test (see Fig. 19). This sudden decrease of pH value is in correlation with the rapid increase of permeability, discussed above. As aforementioned, due to the formation of wormhole, the nitrate solution may flow throughout the sample and as a consequence leading to sharp diminution of pH value in the outlet solution.

5.1. General remarks

In the previous sections, three series of laboratory tests have been performed and presented, namely triaxial compression tests on sound material, asymptotically degraded sample and coupled degradation tests. The results obtained from these tests should provide a useful experimental background for constitutive modelling of chemo-mechanical behaviour in cement paste. Generally, the tests performed on the two specific states, namely sound and degraded states have been conceived as characterization tests to determine basic mechanical behaviour of cement paste and residual behaviour after “complete” chemical lixiviation. For instance, it was found that the basic mechanical behaviour of cement paste can be characterized by two complementary plastic deformation mechanisms, deviatoric shearing and pore collapse. The mechanical responses are strongly pressure sensitive with a transition from brittle to ductile behaviour when the confining pressure increases. However, the volumetric deformation is essentially dominated by volumetric compaction. From these data, an appropriate constitutive model can be formulated. Then comparing the results between the sound and degraded states, the mechanical consequences of chemical degradation may be identified. For instance, the chemical leaching generates a significant increase of material porosity, leading to important diminution of mechanical strength and elastic modulus. The material also becomes more collapsible under compression stresses. These chemical effects should be then introduced in the mechanical model, by considering for example the diminution of pore collapse limit stress. The coupled tests represent a small size boundary values problem under combined mechanical loading and chemical leaching. Therefore, these tests can be used to the first phase of validation of chemo-mechanical model formulated on the basis of tests performed on sound and degraded samples. In particular, these tests should be used to validate the coupling between mechanical deformation and chemical degradation process. For example, comparing the two coupled tests performed under two different values of deviatoric stress; we can observe that the mechanical deformation has also effects on chemical process. In the test with the deviatoric stress of $\sigma_1-\sigma_3=20$ MP$_a$, due to relatively high stress level, the strains induced by chemical leaching is much higher than those in the test with lower deviatoric stress ($\sigma_1-\sigma_3=8$ MP$_a$). Due to this higher deformability, the kinetics of chemical leaching seems significantly smaller in the first test than in the second one (see extension of degraded zones in Fig. 16). It seems that due to high material deformation, the propagation of chemical degradation front is constrained; this may be interpreted by a diminution of diffusion coefficient in chemical process due to mechanical deformation. At the same time, it is also observed that in the test with higher deformation ($\sigma_1-\sigma_3=20$ MP$_a$), the permeability is regularly decreasing due to probably volumetric compaction as mentioned above. While in the test with lower deformation ($\sigma_1-\sigma_3=8$ MP$_a$), the permeability increases slightly but continuously with chemical leaching. Therefore, there is coupling between mechanical deformation and hydraulic properties.

6. Conclusions

Experimental investigations have been presented in the present work in order to study chemical-mechanical behaviours of pure Portland cement paste. The emphasis was put on the porous cement paste under compressive stresses. Three series of laboratory tests have been performed. Triaxial compression tests with different confining pressures have been conducted respectively on sound and degraded materials. It has been shown that the plastic deformation of the porous cement paste may be characterized by two mechanisms: deviatoric shearing and pore collapse. The chemical degradation affects the mechanical behaviour of cement paste by drastic reduction of mechanical strength and plastic yield stresses. In the last part, original coupled chemo-mechanical tests have been proposed. The obtained results in this work may be used in the formulation, identification and validation of chemo-mechanical models. Further, microscopic investigations and deeper chemical analyses of degraded samples would help to better understand physical mechanisms of chemo-mechanical coupling and kinetics of chemical degradation. Of course, more mechanical tests in decoupled and coupled conditions under different stress states will still be useful to constitute larger data base.

Appendix A

Chemical properties of cement used

Chemical compositions	Weight percent (%)
SiO_2	21.29
Al_2O_3	3.45
Fe_2O_3	4.07
CaO	63.51
MgO	2.3
SO_3	2.5
MnO	0.05
TiO_2	0.47
P_2O_5	0.43
K_2O	0.52
Na_2O	0.16
Loss on ignition	0.8
Total	99.55

References

[1] F. Adenot, 1992. Durabilité du béton: caractérisation et modélisation des processus physiques et chimiques de dégradation du ciment. Doctoral thesis (in French), University of Orléans, France.

[2] U. Berner, Evolution of pore water chemistry during degradation of cement in a radioactive waste repository environment, Water management 12 (1992) 201–219.

[3] C. Carde, 1996. Caractérisation et modélisation de l'altération des propriétés mécaniques due à la lixiviation des matériaux cimentaires. Doctoral thesis (in French), INSA Lyon.

[4] A. Delagrave (1996). Study of ingress mechanisms of chloride ions in ordinary and high performance concretes, Ph.D. Thesis, Laval University, Quebec City, Canada, 1996.

[5] B. Gérard, 1996. Contribution des couplages mécanique-chimie-transfert dans la tenue à long terme des ouvrages de stockage de déchet radioactifs. Doctoral thesis (in French), E.N.S. de Cachan and University of Laval.

[6] C. Tognazzi, 1998. Couplages fissuration — dégradation chimique dans les matériaux cimentaires: caractérisation. Doctoral thesis (in French), INSA of Toulouse.

[7] F. Heukamp, F.-J. Ulm, J. Germaine, A. Mechanical properties of calcium leached cement paste: triaxial stress states and the influence of pore pressure, Cement and Concrete Research 31 (2001) 767–774.

[8] F.H. Heukamp, F.-J. Ulm, J.T. Germaine, Poroplastic properties of calcium-leached cement-based materials, Cement and Concrete Research 33 (2003) 1155–1173.

[9] A. Delagrave, M. Pigeon, J. Marchand, E. Revertégat, Influence of chloride ions and pH level on the durability of high performance cement paste, Cement and Concrete Research 26 (1996) 749–760.

[10] U. Schneider, S.W. Chen, The chemo-mechanical effect and the mechano-chemical effect on high performance concrete subjected to stress corrosion, Cement and Concrete Research 28 (4) (1998) 509–522.

[11] O. Bernard, F.-J. Ulm, J.T. Germaine, Volume and deviator creep of calcium-leached cement-based materials, Cement and Concrete Research 33 (2003) 1127–1136.

[12] C. Carde, G. Escadeillas, R. François, Use of ammonium nitrate solution to simulate and accelerate the leaching of cement pastes due to deionized water, Magazine of Concrete Research 49 (1997) 295–301.

[13] M. Mainguy, C. Tognazzi, J.M. Torrenti, F. Adenot, Modelling of leaching in pure cement paste and mortar, Cement and Concrete Research 30 (2000) 83–90.

[14] M. Mainguy, O. Coussy, Propagation fronts during calcium leaching and chloride penetration, Journal of Engineering Mechanics 126 (2000) 250–257.

[15] C. Le Bellégo, B. Gérard, G. Pijaudier-Cabot, Chemo-mechanical effects in mortar beams subjected to water hydrolysis, Journal of Engineering Mechanics 3 (2000) 266–272.

[16] D. Kuhl, F. Bangert, G. Mescheke, Coupled chemo-mechanical deterioration of cementitious materials, Part 1: Modeling, International Journal of Solids and Structures 41 (2004) 15–40.

[17] F.-J. Ulm, E. Lemarchand, H.F. Heukamp, Elements of chemomechanics of calcium leaching of cement-based materials at different scales, Engineering Fracture Mechanics 70 (2003) 871–889.

[18] F. Adenot, Modelling of the corrosion of the cement paste by deionized water, Cement and concrete research 22 (04) (1992) 489–495.

[19] B. Gérard, G. Pijaudier-Cabot, C. Laborderie, Coupled diffusion-damage modelling and the implications on failure due to strain localisation, International Journal of Solids and Structures 35 (1998) 4107–4120.